Original Article

Effect of copper, tungsten copper and tungsten carbide tools on micro-electric discharge drilling of Ti−6Al−4V alloy

Sachin N. Sawant [a], Sachin K. Patil [a], Deepak Rajendra Unune [b,*], Prasad Nazare [a], Szymon Wojciechowski [c,**]

[a] Department of Mechanical Engineering, Rajarambapu Institute of Technology, Rajaramnagar, Shivaji University, Kolhapur 415414, Maharashtra, India
[b] Mechanical-Mechatronics Engineering Department, The LNM Institute of Information Technology, Jaipur − 302031, Rajasthan, India
[c] Faculty of Mechanical Engineering, Poznan University of Technology, 60-965, Poznan, Poland

ARTICLE INFO

ABSTRACT

Achieving microholes with dimensionally higher accuracy on the Ti-6Al-4V alloy using traditional machining techniques is challenging. Micro-electric discharge drilling (μEDD) has become a prominent machining technique in fabricating microholes. Though there are extensive applications of μEDD in producing microholes in difficult-to-cut materials, the appropriate tool materials and process parameters determine the process characteristics and accuracy. Because of the uneven machining and inadequate debris flushing, the technique is less productive and results in high overcut (OC) and hole taper (HT) for the microholes as well as poor material removal rate (MRR). Additionally, the rate of electrode wear affects hole precision. To address these issues, a rotating tool electrode set-up was used to drill microholes in Ti−6Al−4V alloy. The impact of three distinct electrode materials, copper (Cu), tungsten copper (WCu), and tungsten carbide (WC), as well as various process parameters, was investigated. The μEDD was accomplished by changing input process parameters, viz. voltage (V), capacitance (C) and tool rotation speed (TRS) and using Cu, WCu and WC tool electrodes to examine their influence on the process response variables such as MRR, TWR, OC, and HT. The experiments for each electrode were designed using a Taguchi-based L9 array, and the results were examined using Analysis of Variance (ANOVA). Capacitance was found to be the most significant electrical parameter in the μEDD of the titanium alloy. At 10,000 pF capacitance, the WCu electrode showed the highest MRR 0.009247 mm^3/min, which was 6.11% and 21.92% higher than the Cu and WC electrodes. In contrast, the WCu electrode had the lowest tool wear rate (TWR) of 0.002033 mm^3/min, which was 280.61% and 61.61% less than the Cu and WC electrodes, respectively. The WC electrode exhibited more accuracy by reducing the OC and HT compared to the Cu and WCu electrodes. The Cu tool electrode owing to its lower melting point and high thermal conductivity ensued in higher TWR than the WCu and WC

---

* Corresponding author.
** Corresponding author.
E-mail addresses: deepunune@gmail.com (D.R. Unune), szymon.wojciechowski@put.poznan.pl (S. Wojciechowski).
https://doi.org/10.1016/j.jmrt.2023.04.067

electrodes. The used of rotary tool enabled a steady machining and proper flushing of debris. The impact of the tool materials and process variables on the surface quality of manufactured micro-holes was also explored using scanning electron microscopy (SEM) and energy-dispersive X-ray analysis (EDX). The WCu electrode showed higher carbon deposition on the hole surface than the Cu and WC electrodes.

Abbreviations

Adj. SS	Adjusted Sum of Squares
ANOVA	Analysis of variance
DE	Discharge Energy
EDM	Electric Discharge Machining
EDD	Electric Discharge Drilling
ERS	Electrode Rotation Speed
μEDD	Micro Electric Discharge Drilling
EDX	Energy Dispersive X-Ray
EWR	Electrode Wear Rate
IEG	Inter-Electrode Gap
SEM	Scanning Electron Microscopy
HT	Hole Taper
MRR	Material Removal Rate
OC	Overcut
OA	Orthogonal Array
ROC	Radial Overcut
REWR	Relative Electrode Wear Ratio
RWR	Relative Wear Ratio
SCD	Surface Crack Density
AgW	Silver Tungsten
SR	Surface Roughness
TWR	Tool wear Rate
WLT	White Layer Thickness
WR	Wear Ratio

Symbols

Al	Aluminium
θ	Hole Taper Angle
Cu	Copper
C	Capacitance
CuW	Copper Tungsten
D_m	Mean Diameter
D_{ha}	Actual Hole Diameter
D_h	Desired Diameter of Hole
I_d	Discharge Current
τ	Duty Cycle
I	Current
t	Thickness Of The Workpiece
I_p	Peak Current
ρ_w	Density of work material
ρ_e	Density of tool electrode
le	Length Of The Electrode Worn Out
T	Machining time
I	Current
R_a	Surface Roughness
R_t	Radius Of Top Of The Hole
R_b	Radius Of Bottom Of The Hole

T_{on}	Pulse on time
T_{off}	Pulse off time
TRS	Tool Rotation Speed
V	Voltage
V_g	Gap Voltage
W	Tungsten
WC	Tungsten Carbide
WCu	Tungsten Copper

1.   Introduction

The Titanium-based alloys piqued the interest of micro-machining researchers due to their confluence of thermal properties, resistance to corrosion, durability, high operating temperature, and strength-to-weight ratio. Titanium alloys have diversified applications in the areas such as automotive, aircraft, chemical, biomedical and medical implants [1,2]. Because of their exceptional combination of high specific strength (strength-density ratio), fracture-resistant, and corrosion resistance, titanium alloys have a diversity of applications in the aerospace, chemical processing, biomedical, automotive, and nuclear sectors, and conventional machining of Titanium alloys is challenging [3]. Electric discharge machining (EDM) is a thermo-electric unconventional machining technology in which electrical energy is employed to create sparking, and the heat energy of the sparks is primarily responsible for material removal. Electric sparks are produced by the electrode and workpiece once the electrode is maintained at a small distance from the workpiece into the dielectric medium, and voltage is supplied between them. As a result, localized zones of extremely high temperatures emerge, and a small amount of the workpiece material melts and vaporizes in this localized zone. The dielectric liquid circulating across the machining gap carries away most debris particles formed due to melted material from the inter-electrode gap (IEG). The μEDD is a version of the same process for micromachining that uses pulse energies between 1 and 10 J [4]. The μEDD is an effective process capable of producing holes ranging in size from a few microns to a few mm irrespective of material toughness [5]. The electrode revolves in μEDD to deliver more significant flushing, causing consistency in the created hole profile.

From the standpoint of many manufacturing industries, the research study is focused on the unique production of microholes in titanium alloys is of utmost importance. In a diversified industry, including aerospace, automotive,

healthcare, nuclear, chemical, and marine, the holes should meet the requirement of the products and are suitable for assembling and disassembling and for routine maintenance. The input factors, including capacitance, voltage, and TRS, primarily control the µEDD process. In addition, factors including the type of dielectric fluid, flushing mechanism, and workpiece and tool materials impact the micro-holes characteristics. Ishfaq et al. [6] performed the experimentation with WC, Cu and graphite electrodes using Taguchi L18 array with relative MRR and SR as output responses. It was found that WC electrode exhibited minimum SR compare to Cu and graphite electrodes. Dewangan et al. [7] examined the influence of various electrode materials such as Cu, brass and graphite and different machine variables such as discharge current (I_d), pulse on time (T_{on}), duty cycle (τ), and polarity on surface quality EDM machined workpiece. The graphite tool produced the highest white layer thickness (WLT), surface crack density (SCD), and surface roughness (SR). The Cu tool exhibits low SR as compared to graphite and brass electrode. The WLT and SR were not considerably impacted by the τ and T_{on}. Lee and Li [8] investigated the effect of electrode materials like graphite, copper tungsten (CuW) and Cu on the MRR, relative wear ratio (RWR) and the SR in EDM of WC. Compared to Cu and graphite, the CuW electrode has a relatively low wear ratio and a superior surface quality; the graphite electrode seems to have a higher MRR, followed by CuW and Cu electrodes. Singh et al. [9] examined the effect of electrode materials (Cu, CuW, brass, and aluminium (Al)) and current (I) on MRR, OC, TWR, and SR in EDM of En-31 tool steel. Cu and Al electrodes exhibit high MRR with a high value of SR. Whereas Cu and CuW offer low electrode wear rate (EWR). Brass electrodes show high wear. Ishfaq et al. [10] investigated the influence of various dielectric mediums (kerosene oil, transformer oil, and canola oil), powders (alumina, graphite, and silicon carbide), and electrodes (copper, brass, and aluminium) for the fabrication of micro-impressions in AISI 316 using EDM. MRR and TWR were found to be significantly enhanced when machining was performed using a silicon carbide mixed kerosene dielectric against a silicon carbide aluminium tool at a pulse time ratio of 1.5. Zhu et al. [11] examined the high-speed EDM of W9Mo3Cr4V graphite electrode, which gives high MRR and relative electrode wear ratio (REWR). In the EDM, along with electrode materials, polarity, peak current (I_p), discharge gap, and discharge time affects the machining performance of EDM. Mouli et al. [12] examined the influence of Cu and graphite electrodes on the EDM of M2 high-speed steel. The graphite tool electrode resulted in a 12.84% greater MRR and an 11.59% smaller SR than the Cu tool electrode. Cu electrode caused a 3.61% lesser EWR. Haron et al. [13] studied the effect of Cu and graphite electrodes in the electrical-discharge machining of XW42 tool steel. They have investigated the machining of XW42 tool steel at two different current values (3 A and 6 A) and in three different diameters (10, 15 and 20 mm). They discovered that the Cu electrode had a greater MRR and a substantially low EWR than the graphite electrode. The EWR and MRR were lowered when the current and electrode diameter increased. The machining of the titanium alloy Ti−5Al-2.5Sn was tested using various electrode types, including zinc, brass, and Cu. The response characteristics were measured by SR, SCD, radial overcut (ROC), and

recast layer for the T_{on}, gap voltage (V_g), I_p, and τ. Cu electrode is found to have the best surface quality and the least amount of ROC, followed by brass and zinc electrodes. In addition, compared to brass and zinc electrodes, the EDMed surface machined by the Cu electrode had a thin and more uniform recast layer and a greater SCD [14]. S. Zahoor et al. [15] studied the effect of cutting speed, feed per flute and axial depth of cut on SR, surface topography, microhardness, white layer formation and residual stresses in milling of IN718 alloy. It was concluded that the use of a biodegradable cutting fluid-based flooding cooling approach has the potential to improve the surface integrity of IN718. Chaudhary et al. [16] have studied the characteristics of the EDMed SS316 using MRR and SR with varied electrode, T_{on} and current (I). The effect of electrode materials (Cu, brass, and graphite), I and T_{on} have been studied for the EDM process. The impact of input factors on output response MRR and surface quality were examined for hardened steel 316. It is found that MRR rises with I_d. Therefore, Cu electrodes have better MRR than brass and graphite electrodes. As T_{on} increased, MRR also increased. Surface finish is influenced mostly by the electrodes, then I_d and lastly by T_{on}. In EDM turning of the titanium alloy, Rex and Vijayan [17] have investigated the influence of the I_p, T_{on}, pulse off time (T_{off}), on MRR, TWR, diametrical accuracy and SR with Taguchi design of experiments using L9 orthogonal array (OA). The optimum parameters found using GRA in the experimentation showed a 127% enhancement in MRR and a 45.3% drop in SR. Ishfaq et al. [18] carried out experimentation using three different electrodes Cu, Brass and graphite against five types of dielectric media. Cryo-treated graphite electrodes provided the highest MRR when Tween-20 mixed with kerosene was used as the dielectric medium. It was also discovered that Span-20 added kerosene is the perfect option for achieving high MRR while using non-deep cryogenic treated electrodes, whilst Tween-20 combined kerosene is best suited for Cryo-treated electrodes. Urso and Merla [19] examined the influence of tool materials like Cu, Brass and tungsten (W) with different shapes (cylindrical and tubular) in the µEDD of Stainless Steel and Titanium. The W electrode showed the best TWR than brass and Cu. For steel and brass material, the cylindrical electrode shape showed a lower TWR. However, for titanium and magnesium workpieces, tubular-shaped electrodes showed lower TWR. Sen and Mondal [20] examined the impact of the input factors on MRR, EWR and surface finish in EDM of mild steel grade IS2062 using various electrode materials like Cu, brass and graphite. They observed that graphite showed the highest MRR than Cu and brass. However, in the case of TWR, capacitance and brass have shown quite low compared to graphite, which yields better results than Cu and brass. The brass electrode showed a good surface finish, and graphite showed a very high SR value. Urso et al. [21] investigated the influence of various electrode materials, like brass and WC, for fabricating holes in Stainless Steel and WC with EDM. For brass and WC electrodes, I_p and V are proportional to MRR and TWR. In EDM drilling of the WC and stainless steel, the WC electrode performed better than the Brass electrode. Owing to its better electrical conductivity and higher discharge energy (DE) usage, the brass electrode has a greater TWR than the WC electrode. The influence of various electrodes like Cu, CuW, and graphite on the machining of 17-4 PH

Table 1 – Overview showing the effect of various electrode materials on the capabilities of μEDD.

Reference	Electrode Material	Workpiece	Machine Parameters	Response variables	Observations
Joy et al. [29]	Carbide Tool coated with TiAlN Diameter	Ti–6Al 4V	Spindle Speed, Feed rate and drill diameter	TWR, Cutting Force Chip formation	Tool wear in the drilling of Titanium is extremely significant to deviations in feed rate
Zhu et al. [30]	Solid carbide	Ti–6Al 4V	Cutting speed Feed rate	Cutting force, Hole accuracy, chip formation	Thrust force increases with feed rate. The feed rate selection has an important impact on the shape and size of the chips.
Mondol et al. [31]	W	Ti–6Al 4V	V, C, Threshold %	MRR, TWR, Wear Ratio (WR), OC and HT	MRR and TWR increase with C and V
Barman et al. [32]	W	Ti–6Al 4V	V_g, C, depth of the hole	Surface finish	Surface finish decreases with a rise in the V_g, C
Rahul et al. [33]	W and Cu	Ti–6Al 4V	V_g, T_{on}, τ, flushing pressure, Polarity, Gap	MRR, Surface Finish, SCD, WLT	Cryogenically treated W electrode showed better performance than an original electrode
Yadav and Yadava [27]	Cu	Ti–6Al–4V	I, T_{on}, τ, and ERS	Hole Accuracy and SR	Electrode Speed effects the surface finish and Hole accuracy
Plazaa et al. [34]	Helical Shaped Graphite and CuW electrode	Ti–6Al–4V	Hole Depth, T_{on}, Pulse off Time (T_{off})	MRR and Electrode Wear	Graphite electrode depicts more MRR and TWR than CuW electrode
Ahmada and Lajis [35]	Cu	Inconel 718	I_p, Pulse Duration	MRR, EWR and SR	MRR and EWR increase with I_p and pulse duration.
Urso et al. [21]	Brass and WC	WC and Stainless steel (AISI 304)	I_p, V, and Frequency	MRR, TWR and DOC	MRR and TWR grow as process parameters are increased
Unune et al. [23]	W	Inconel 718	V_g, C, Feed rate, ERS, and Vibrational frequency	MRR, EWR, OC, HT, surface quality	Low-frequency vibration aid to the workpiece increased EDD performance
Moses and Jahan [36]	WC	Brass and Ti–6Al–4V	V, C, TRS	Dimensional accuracy, Surface Quality	Better dimensional accuracy and surface finish were observed in the brass as compared to Ti–6Al–4V
Prasanna et al. [37]	WCu	Ti–6Al–4V	V_g, I_p, T_{on} and τ	MRR and TWR	MRR and TWR rises with the rise in V, I and T_{on}
Urso, and Merla [19]	Cu, Brass and WC	Stainless steel, Titanium, Magnesium brass	I_p, V, Electrode material, Electrode Geometry, Workpiece material	TWR, conicity and diametrical OC	WC Electrode exhibits less TWR and OC as compared to brass and Cu
Mustafa Ay et al. [38]	CuW	Inconel 718 Alloy	I_d, Pulse duration	HT and hole dilation	HT and dilatation rise with a rise in I_d and pulse duration
Dewangan et al. [39]	Cu	Ti–6Al–4V Alloy	C, V, T_{on} and TRS.	Surface Texture, OC and MRR	For both MRR and OC, C is the most influential component in the μEDM process

Table 2 − Chemical composition of Ti−6Al−4V.									
Constituents	Ti	Al	V	Mn	C	N	Cu	Fe	Cr
Composition	89.389	6.131	4.199	0.004	0.019	0.043	0.023	0121	0.015

and 316 L steel using EDM was investigated. In EDM of 316 L and 17−4 PH materials, the Cu electrode exhibits a greater MRR than graphite. However, CuW offers a low MRR. The CuW offered low diametrical overcut, good dimensional accuracy and low values of SR for 17-PH and 316 L steel [22]. Unune et al. [23] examined the effect of the voltage, capacitance, electrode rotation speed (ERS) and vibrational frequency on MRR, TWR, OC and HT for Inconel 718 alloy using the W electrode. The effectiveness of low-frequency vibration-aided μEDD has been enhanced due to better flushing, debris removal, and steady machining conditions. Sapkal and Jagtap [24] optimized the process using multiobjective optimization technique and found that MRR is influenced by the discharge voltage, capacitance and ERS. While taper ratio influenced by the pulse on time and capacitance. Hascalık and Caydas [25] experimentally investigated the surface quality of EDMed Ti−6Al−4V by using various electrodes such as electrolytic Cu, graphite, and Al electrode and altering machining parameters. They discovered that increasing the current and pulse time improved responses like surface finish, MRR, EWR, and WLT. Jahan et al. [26] examined the surface finish in the μEDM of the WC with W, CuW and silver tungsten (AgW) electrodes. They observed that the surface finish is greatly affected by the DE while machining and the electrical and thermal characteristics of the electrodes. It was discovered that AgW electrodes generate a smoother surface, CuW electrodes have the highest MRR, and W cvcgdnn'a electrodes have the lowest wear. Yadav and Yadava [27] demonstrated the advantages of EDD operation over stationary tool electrodes for producing holes in titanium alloy workpieces with electrolytic Cu electrodes. It is discovered that rotating electrode machining has a considerable impact on responses such as hole circularity and SR when compared to stationary electrode machining. Yilmaz et al. [28] built an automated system for EDD operation on two different aerospace alloys with Cu and brass electrodes with 11 variations in diameter. A collective response optimization approach was applied to establish the best circumstances for EDD. The ANFIS model was created utilizing machine parameters and responses to give a better forecast.

In light of the above-mentioned review of the widespread use of various tool electrode materials in EDM and μEDD in Table 1., the Cu, WCu, and WC materials were chosen as electrode materials in the present study of μEDD in Ti−6Al−4V alloy. The following were the primary reasons for selecting these electrode materials.

i) The most significant factor is that the chosen materials have a high MRR. According to the literature, Cu and WC material have a higher MRR due to their high melting points. Furthermore, WC can produce a good surface finish.
ii) These electrodes are inexpensive and widely accessible on the market. According to a literature review, the electrode material has a considerable influence on the machining indices of μEDD.

The proper tool material selection is crucial in creating holes with μEDD effectively. However, little research is available comparing the machining performance characteristics of various electrode materials. Furthermore, only a few studies discovered the impact of input electrical parameters (like V, C, and TRS) on machining performances. Moreover, no research has been stated for measuring machining performance and comparing the μEDD of Ti−6Al−4V alloy utilizing various electrode materials. However, the influence of different electrode materials and machining parameters on machining performances in the μEDD of Ti−6Al−4V alloy must be examined. This research used the μEDD to investigate the performance of various tool electrode materials at different machine parameter values on MRR, TWR, OC, and HT measures in μEDD of Ti−6Al−4V material. Furthermore, SEM and EDX were used to investigate the microscopic images of generated hole surfaces obtained using various electrodes and transfer of electrode materials and workpiece elements.

2.   Materials and methods

2.1.   Material for the experiment

Ti−6Al−4V (grade 5) alloy with a dimension of 50 mm × 50 mm x 1 mm was obtained from Sachin Steel Centre in Mumbai for the experiment. Table 2 shows the chemical composition of the Titanium Grade 5 alloy, and Table 3 presents its mechanical characteristics. The properties of selected tool materials are listed in Table 4.

The workpiece sample after polishing and grinding by the polishing machine used in the experiment (MetaServ-250, Buehler USA).

2.2.   Experimental set-up and measuring apparatus

The μEDD was carried out using the versatile machine tool (DT110; Mikrotools Singapore) depicted in Fig. 1. The commercially available "TOTAL DIEL7500IN" was used as dielectric oil. The Ti−6Al−4V specimen was firmly fixed onto the fixture at a right angle to the electrode of Ø500 μm. The set-up for experimentation of the μEDD of Ti−6Al−4V is shown in Fig. 1. Three various electrode materials, Cu, WCu and WC of

Table 3 − Mechanical properties of Ti−6Al−4V.	
Property	Value
Hardness HV$_{20}$	600
Melting Point (°C)	1660
Ultimate tensile Strength (MPa)	832
Yield Strength (MPa)	745
Impact Toughness (J)	34
Elastic Modulus (GPa)	117
Thermal Conductivity (W/m °C at 200 °C	7.2

Table 4 — Selected tool electrode material properties.

Property	Cu	WCu	WC
Composition	99.99% Cu	80% W and 20% Cu	WC 94 Co6
Melting Point (°C)	1045	3280	2867
Density gm/cm³	8.96	15.9	14.8
Electrical Resistivity (μΩm)	169	45	20
Electrical Conductivity (10^6 S/M)	58.5	43	18
Thermal Conductivity (W/m K)	391	220	70

diameter 500 μm, were used for the drilling of titanium grade 5 alloy. The selected control factors are voltage, capacitance and TRS. For each electrode, an L9 OA based on the Taguchi design was implemented for three levels of each input parameter. Table 5 shows the details of the machining conditions for the experimental trials. Each experiment was performed with a fresh dressed tip of tool electrode. The experimental procedure followed for this work in given below.

i. Secure the prepared workpiece in the DT110 machine tool's workholder and ensure that it is properly aligned.
ii. Prepare the electrode: Choose an electrode material e.g. Cu, WCu and WC. Attach the electrode to the DT110's electrode holder (collet).
iii. Start the dielectric supply.
iv. Set the machining parameters: Set the input machining parameters as per required experimental run.
v. Start the drilling process: With the workpiece and electrode in place and the machining parameters set, start the μEDD process by energizing the electrode with a series of short, high-energy electrical pulses. The dielectric fluid will ionize and form a plasma channel between the electrode and the workpiece, which will erode the workpiece material and create the desired hole.

vi. Monitor the process: Monitor the drilling process closely to ensure that the hole is being drilled to the desired dimensions and that the electrode is not breaking.
vii. Finish the drilling process: Once the desired hole has been drilled, stop the μEDD process.
viii. Dressing of tool electrode tip: The worn out the tool electrode tip is dressed so that new tip is available for next experimental run.

Following the experimentations, the manufactured microholes were examined using a Digital Microscope (Axio Cam AX10; ZEISS Germany) with a 20x lens. Axio Cam Software was used to determine the radius of the hole. Images captured with the SEM (JSM-IT 200; JEOL, USA) at 500X microscopy were used to assess the surface properties of microholes.

2.3. Experimental measurements

To assess the performance of the μEDD while machining Ti—6Al—4V, the MRR, TWR, surface texture, and precision level (related to OC and HT) of microholes were measured. The MRR, EWR, OC, and HT were calculated using the following equations:

The volumetric material removal rate of the machined surface throughout actual machining is denoted by MRR. It is expressed in mm³/min. It is an essential measure of the μEDD. Eq. (i) determined the MRR,

$$MRR = \frac{\pi Dm^2}{\rho_w \times 4 \times T} \times t \tag{i}$$

where,

$$Mean\,Diameter\,(Dm) = \frac{Top\,Diameter\,of\,Hole + Bottom\,Diameter\,of\,Hole}{2} \tag{ii}$$

where, t is the thickness of the workpiece, ρ_w is the density of the workpiece in g/mm³, and T is the machining time recorded in minutes.

(a)   *(b)*
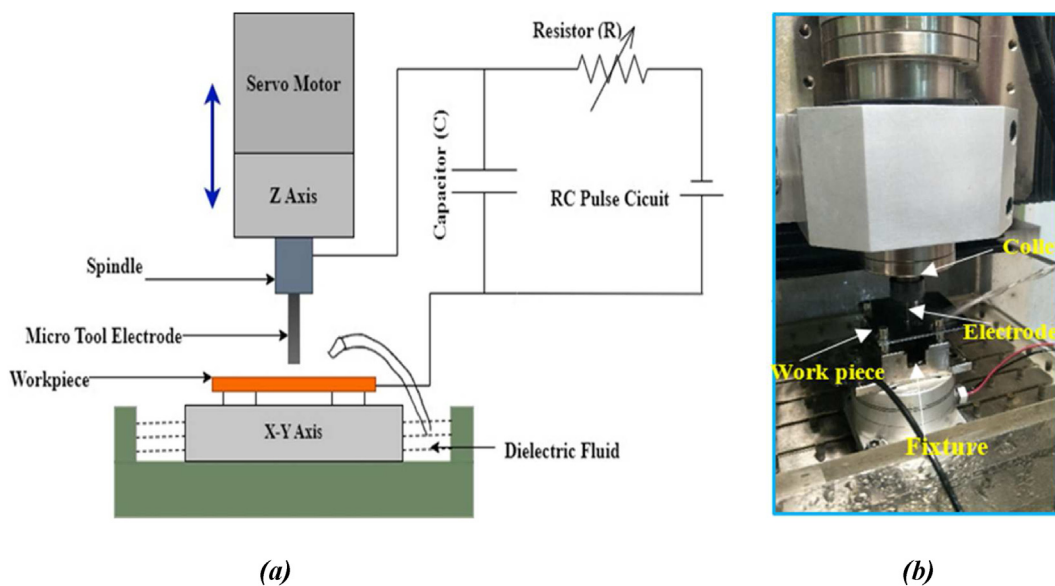
Fig. 1 — Experimental setup (a) Schematic diagram; (b) photograph of Micro-electro discharge drilling on DT110 machinetool.

Table 5 – Machining conditions.

Item	Description
Tool (Cathode)	Cu, WCu and WC
Workpiece (Anode)	Ti−6Al−4V (50 × 50 × 1 mm)
Dimensions	Φ 500 μm
Dielectric medium	TOTAL DIEL7500IN
Number of Experiments	9 for each electrode using Taguchi L9 OA (Total 27 experiments)
Control factors	Voltage (V), Capacitance (pF) and ERS (RPM)
Responses	MRR (mm³/min), TWR (mm³/min), OC (mm) and HT (degree)

Table 6 – Input factors and their levels.

Control parameters	Levels			Unit
	1	2	3	
Capacitance	100	1000	10,000	pF
Voltage	80	100	120	V
Tool Rotation Speed	0	500	1000	RPM

3.1. Analysis of Variance

The influence of process parameters for each tool electrode on the MRR, TWR, OC and HT was tested using ANOVA, and the findings are shown in Table 8. ANOVA was performed with 95% confidence level. The stochastic significance of the parameter is represented by P-value. When the P-value of an input factor is lower than 0.05, it substantially influences the response [40,41]. The variation in the output response variable mentioned by each model term is summarised by the adjusted sum of squares (Adj. SS). According to the table, capacitance is the most influential parameter for MRR, TWR, OC, and HT, accounting for a contribution of 50%, 71.43%, 48%, and 51%, respectively, for the Cu tool electrodes. Similarly, for the WCu electrode, the capacitance was found to be a crucial factor for MRR, TWR, OC, and HT, which contributed 53.33%, 71.42%, 47.93%, and 69.84%, respectively. In addition, in the case of the WC tool, the capacitance was found to be the most substantial factor affecting the MRR, TWR, OC, and HT by 54.28%, 74.07%, 44.57%, and 68.91%, respectively.

In this research study, the TRS was the second most significant factor for MRR and OC, while the voltage was the second most crucial factor in the case of TWR and HT. For the Cu electrode, TRS contributed 44.44% and 32.95% to MRR and OC. For the WCu electrode, TRS significantly affects MRR and OC, contributing 40.00% and 35.26%, respectively. TRS considerably affected the MRR and OC in the context of the WC electrode, contributing 27.14% and 38.30%, respectively. For TWR and HT, the voltage was the second-highest influencing factor for the Cu electrode, contributing 23.08% and 41.85%, respectively. Likewise, for WCu electrode, the voltage was the second significant factor in influencing TWR and HT and contributing 28.28% and 14.28%, respectively. For WC, the voltage was the most crucial parameter in determining TWR and HT and showed contributions of 18.52% and 30.55%, respectively.

TWR is the rate of electrode wear during the drilling operation, expressed in mm³/min. It is a critical response variable that influences machining cost and precision level. The electrode length was measured after every hole using the Z-axis coordinate of the machines. The diameter of the electrode is 500 μm. The TWR formula is given in equation (iii),

$$TWR = \frac{\pi D t^2}{\rho_e \times 4} \times l e \qquad (iii)$$

Here, ρ_e is the density of the electrode in g/mm³, and l_e is the length of the electrode worn out.

The OC of the hole serves as the most important criterion for assessing hole precision. The OC was calculated using Eq. (iv),

$$OC = D_{ha} - D_h \qquad (iv)$$

where D_{ha} is the actual hole diameter measured using a 3D profilometer and D_h is the desired diameter of the hole.

The HT angle (θ) was determined using Eq. (v),

$$\theta = \tan^{-1}\left(\frac{R_t - R_b}{t}\right) \qquad (v)$$

where, R_t and R_b are the radii of the top and bottom of the hole.

2.4. Design of experiments

The design of experiment in this study was conducted utilizing the Taguchi approach. The experiment was carried out to ascertain the impact of various electrode materials and processing variables μEDD's performance. Each electrode material, Cu, WCu, and WC, was subjected to nine experiments. A Taguchi L9 OA with three process variables at three levels was used for this study. Table 6 displays the voltage, capacitance and TRS at three levels. Table 7 depicts the measured response measured for the selected experimental design.

3. Result and discussions

The influence of tool material and input parameters on various responses such as MRR, TWR, OC and HT was examined for μEDD in Ti−6Al−4V alloy. The following section discusses the ANOVA study as well as the influence of individual input factors using the mean plot for each electrode.

3.2. Effect of process parameters on μEDD performance

Using μEDD for drilling Ti−6Al−4V alloy, various process parameters and their effect on the MRR, TWR, OC and HT were assessed. From ANOVA analysis, the significant process parameters were identified, and then the mean effect charts were produced and presented in this section.

3.2.1. Effect of voltage

Fig. 2 shows the mean effect plots representing the influence of the voltage on the MRR, TWR, OC and HT. As the voltage increased from 80 V to 120 V, MRR was seen to rise. The WCu electrode shows a higher MRR than Cu and WC electrodes. The WCu electrode shows a maximum MRR of 0.008007 mm³/min

Table 7 — Responses measured for three electrodes.

Run	Input parameters			For Cu				For WCu				For WC			
	V	C	TRS	MRR	TWR	OC	HT	MRR	TWR	OC	HT	MRR	TWR	OC	HT
				mm^3/min	mm^3/min	mm	Degrees	mm^3/min	mm^3/min	mm	Degrees	mm^3/min	mm^3/min	mm	Degrees
1	80	100	0	0.00019	0.00024	0.00308	0.89783	0.00020	0.00010	0.00252	0.69783	0.00024	0.00017	0.0015	0.53678
2	80	1000	500	0.00467	0.00209	0.00682	0.76540	0.00497	0.00070	0.00553	0.67540	0.0035	0.00126	0.0034	0.49540
3	80	10,000	1000	0.00966	0.00506	0.01002	0.56367	0.00986	0.00087	0.0088	0.36367	0.00781	0.00277	0.0077	0.38367
4	100	100	500	0.00386	0.00221	0.0155	0.48029	0.00406	0.00020	0.01008	0.35030	0.0025	0.00162	0.0097	0.26995
5	100	1000	1000	0.00746	0.00478	0.0098	0.30980	0.00786	0.00099	0.00891	0.21980	0.00649	0.00126	0.0075	0.19800
6	100	10,000	0	0.00646	0.00854	0.09845	2.73034	0.00686	0.00273	0.092	2.23034	0.00523	0.00539	0.0793	2.03034
7	120	100	1000	0.00652	0.00098	0.00562	0.40514	0.00692	0.00025	0.00401	0.32514	0.00627	0.00055	0.0031	0.25144
8	120	1000	0	0.00587	0.00754	0.0965	2.22353	0.00606	0.00175	0.091	2.00353	0.00384	0.00514	0.072	2.00353
9	120	10,000	500	0.01003	0.00961	0.09275	2.63500	0.01103	0.00248	0.08421	2.32150	0.00972	0.00620	0.0694	1.98321

showing a 59.75% rise. The MRR related to Cu and WC electrodes increased by 54.34% and 71.65% for the voltage variation of 80 V—100 V. The MRR rises as the voltage rises because it is proportional to the spark energy. A similar trend was observed for the TWR depicted in Fig. 2. (b) For Cu, WCu, and WC electrodes, TWR values increased by 145.33%, 165.27% and 183.21, respectively. Because of its low melting point and excellent heat conductivity, Cu electrodes have the greatest TWR, measuring 0.006045 mm^3/min. The TWR has grown as both the voltage and the capacitance have increased, although the TWR is very capacitance-sensitive. Capacitance is the most crucial facet of micro-EDM since it controls charging and discharging.

The influence of voltage on OC is illustrated Fig. 2. (c). The WC electrode has shown a 1043.26% rise in the OC value for the voltage range of 80 V—120 V. The Cu electrode shows an OC value of 0.06498, which is 8.73 and 34.83% higher than the WCu and WC electrodes. A lower DE is better suitable for the smaller OC because DE is proportional to voltage. The Cu electrode melts easily because the lower melting point causes material deposition on the tip, which can increase the diameter of the hole. Due to their high melting points and poor conductivities, WCu and WC haven't had material deposited on the tool's tip. At a high voltage, higher MRR decreases flushing effectiveness and increases the chance of arcing, which results in more OC.

Fig. 2 (d) describes the effect of the voltage on the HT. For HT, the trend is the same as for OC. The Cu electrode displayed the highest HT value of 1.7546° compared to the WCu and WC electrodes. Voltage has a significant effect on increasing the HT. Owing to the secondary spark produced in the IEG, the HT rises with voltage.

3.2.2. Effect of capacitance

Fig. 3 depicts the influence of capacitance on the response variables. The graphs prove that MRR, TWR, OC and HT rise with a rise in the capacitance level. The DE generated in the RC pulse circuit is a function of capacitance and voltage (DE = 1/2 CV^2). As a result, the capacitance value determines the degree of DE. As a result, the MRR will be higher at a higher capacitance value [42]. The MRR increased from 0.003522 mm^3/min to 0.008714 mm^3/min for a change of the capacitance from 100 pF to 10000 pF, showing a 147.41% rise in the case of the Cu electrode. Likewise, the MRR was improved by 147.97% and 152.63% for the WCu electrode and WC electrode, respectively. This research found that the MRR is far more sensitive to capacitance and TRS than voltage. When compared to Cu and WC tool electrodes, drilling Ti—6Al—4V alloy using the WCu electrode has produced the highest MRR. This high MRR is made possible by the WCu electrode's poorer thermal conductivity, which absorbs less heat produced so that most heat is available for the material removal from the titanium alloy. The maximum MRR at 10000 pF was demonstrated by a WCu electrode with a reading of 0.009247 mm^3/min, which was 6.11% greater than Cu and 21.92% more significant than a WC tool electrode.

Fig. 3 (b) shown that the Cu electrode exhibited the highest TWR of 0.007738 mm^3/min, 280.62% more than the WCu electrode and 61.61% more than the WC electrode. TWR is low for tool electrodes with the highest melting point and low

**Table 8 – Results of the ANOVA for MRR, TWR, OC, and HT.**

Factor	For Cu			For WCu			For WC		
	Adj. SS	P-Value	Percentage Contribution	Adj. SS	P-Value	Percentage Contribution	Adj. SS	P-Value	Percentage Contribution
MRR									
V	0.000011	0.06	15.28	0.000014	0.019	17.07	0.000012	0.071	18.461
C	0.00004	0.02	55.56	0.000046	0.006	56.10	0.000032	0.027	49.23
TRS	0.000021	0.03	29.17	0.000022	0.012	26.83	0.000021	0.041	32.30
TWR									
V	0.000021	0.093	23.08	0.000001	0.09	14.28571	0.00001	0.093	24.39
C	0.000065	0.032	71.43	0.000005	0.027	71.42857	0.000024	0.04	58.54
TRS	0.000005	0.298	5.49	0.000001	0.126	14.28571	0.000007	0.132	17.07
OC									
V	0.005161	0.009	33.62	0.004426	0.008	32.47	0.002971	0.007	31.75
C	0.005223	0.009	34.03	0.004736	0.007	34.74	0.003368	0.006	35.99
TRS	0.004966	0.009	32.35	0.00447	0.008	32.79	0.003019	0.007	32.26
HT									
V	1.54824	0.05	19.38	1.44886	0.039	23.03	1.35161	0.002	24.40
C	2.93358	0.027	36.72	2.10466	0.028	33.45	1.85842	0.001	33.55
TRS	3.50765	0.023	43.90	2.73806	0.021	43.52	2.32868	0.001	42.04
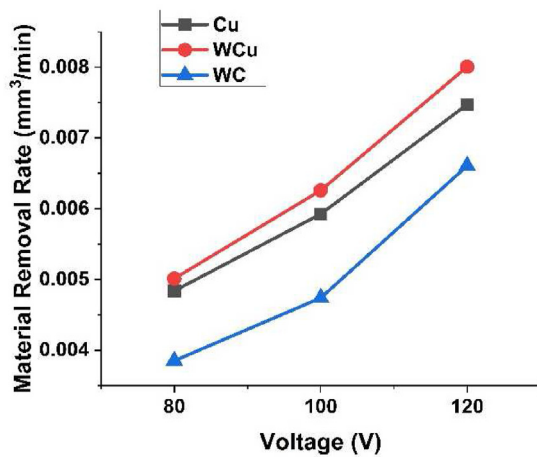
(a)
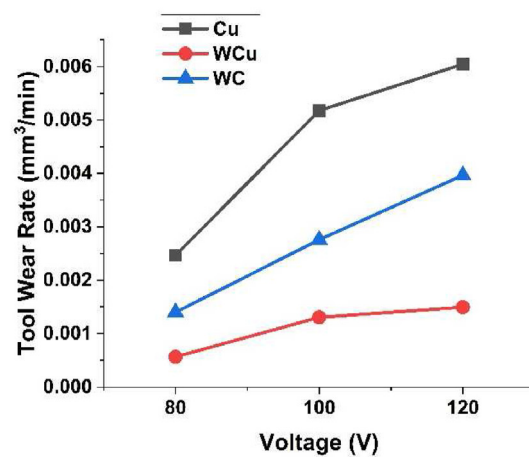
(b)
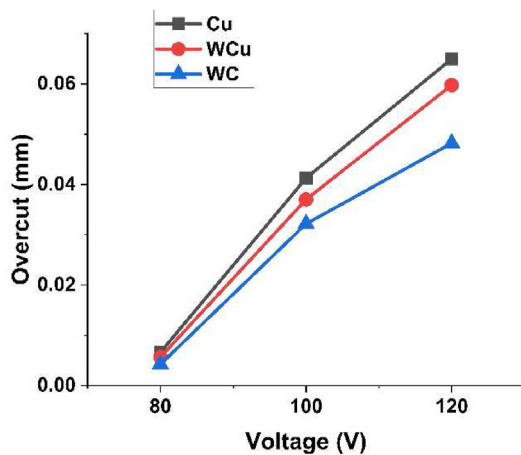
(c)
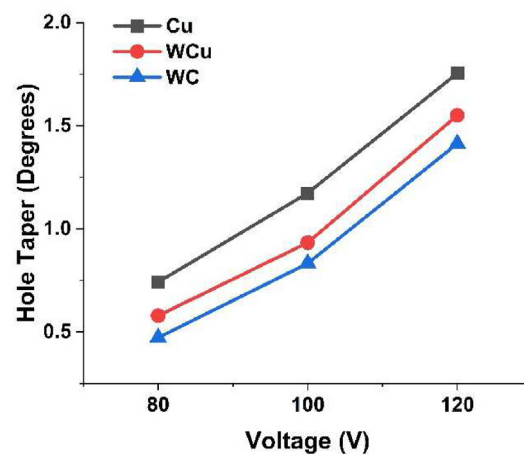
(d)

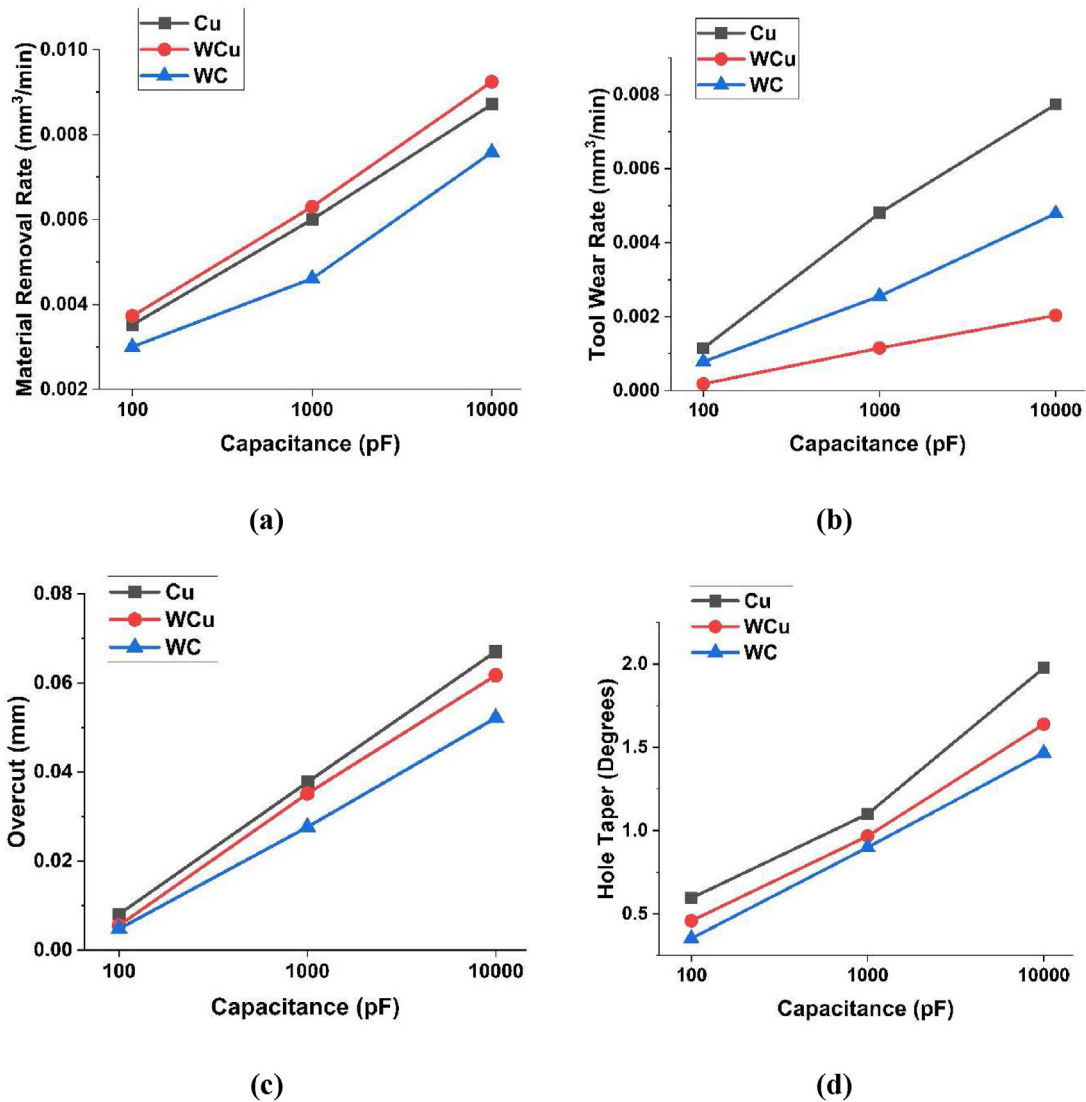Fig. 2 – Influence of the voltage on (a) MRR, (b) TWR, (c) OC and (d) HT.

Fig. 3 − Influence of the capacitance on (a) MRR, (b) TWR, (c) OC and (d) HT.

thermal conductivity [43]. WCu and WC have a higher melting point and lower thermal conductivity than Cu, resulting in lower TWR. The electrode with low melting and higher thermal conductivity melts due to heat produced in the (IEG). Due to its higher melting point and lower thermal conductivity, the WCu electrode has excellent wear resistance.

The OC affects a workpiece's ability to achieve better dimensional precision as well as finishing. The plots from Fig. 3. (c) Depict that OC value rises with the capacitance value for all the tool materials. The Cu and WCu tool electrode shows a large amount of OC, 0.06707 mm and 0.061702 mm, respectively. In contrast, the WC electrode exhibits an OC of 0.0805 mm. The OC increased by 731.46%, 1014.35% and 993.19% for the Cu electrode, WCu and WC electrode, respectively, for the capacitance variation from 100 pF to 10000 pF. It can be concluded that a more significant amount of DE is not suitable for producing the lower OC. At higher discharge energies, a larger workpiece volume is ejected per discharge, resulting in more craters and debris and a higher OC. Furthermore, a discharge column constructed at a higher

DE and maintained for a prolonged period of time than one built at a lower DE causes a more significant ionization effect and enlarged microholes [44].

The plot from Fig. 3 (d) represents the influence of capacitance on the HT. As the capacitance value rises, the HT also rises. The Cu electrode showed the highest taper value of 1.9763°, with 1.6385° and 1.4657° for WCu and WC electrodes, respectively. For Cu, WCu and WCu electrodes, the HT increased by 232.48%, 257.90% and 315.56%, respectively, for the capacitance variation from 100 pF to 10000 pF. Because of the increased DE, large and deep craters form, resulting in short circuits and arcing into the secondary sparking. The Cu electrode has more excellent electrical conductivity and low melting point than the WCu and WC, the reason behind this highest HT produced.

3.2.3. Effect of TRS
The plots from Fig. 4 depict TRS's effect on MRR, TWR, OC, and HT for various electrode materials. Fig. 4 (a) exhibits that the MRR increased for all tool electrode materials as TRS
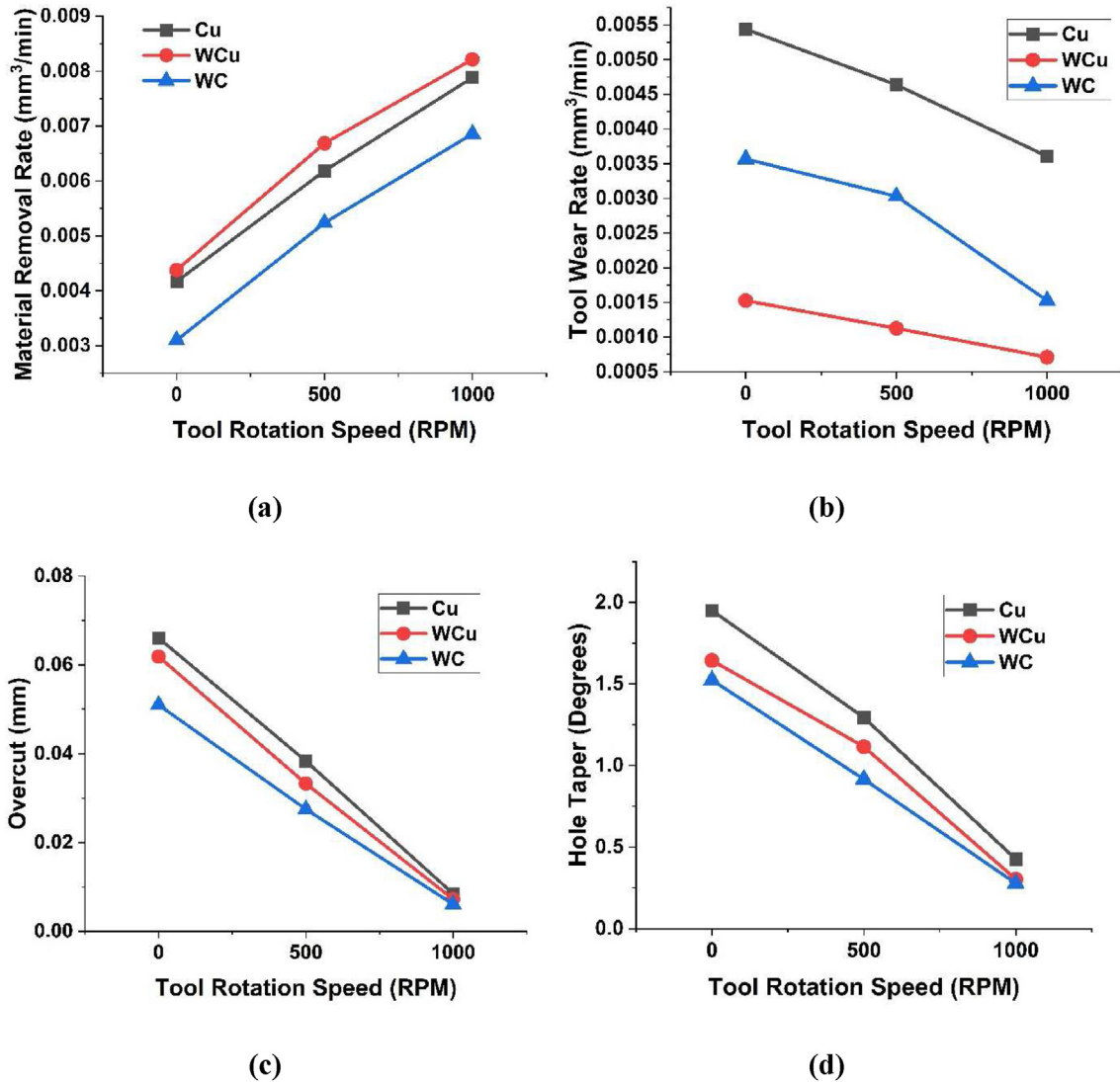
Fig. 4 − Effect of the TRS on (a) MRR, (b) TWR, (c) OC and (d) HT.

risen from 0 to 1000 rpm. The WCu electrode achieved the highest MRR than WC and Cu electrodes. The MRR for the WCu electrode is increased from 0.00417 mm³/min to 0.007881 mm³/min, representing an 88.99% rise as TRS is varied from 0 to 1000 rpm. Similarly, for TRS variations from 0 to 1000 rpm, the MRR increased by 87.68% and 121.22% for Cu and WC tool electrodes, respectively. The flushing of debris from the inter-electrode space is adequately done due to the greater TRS [42].
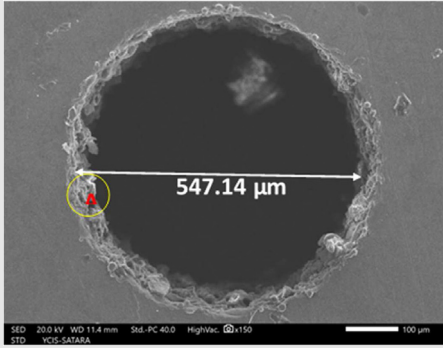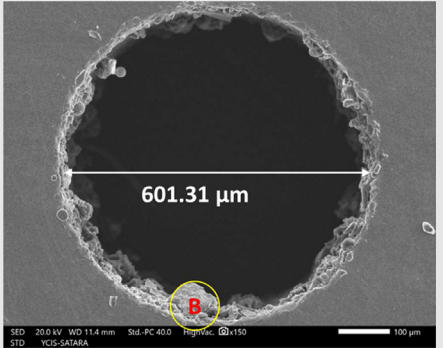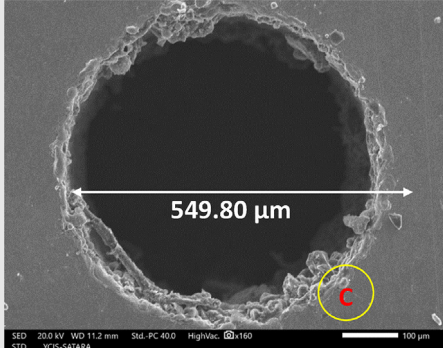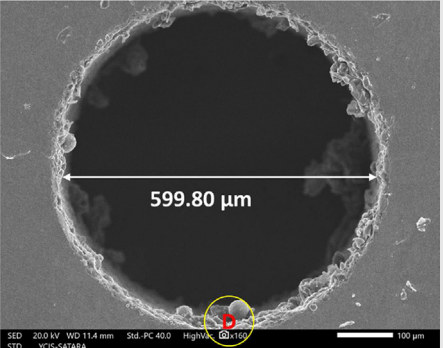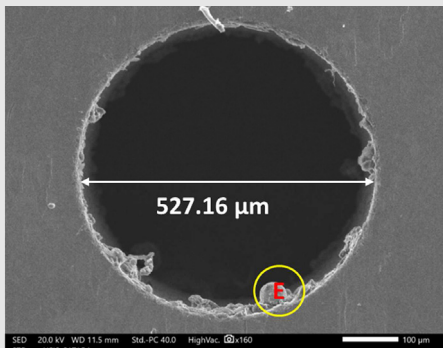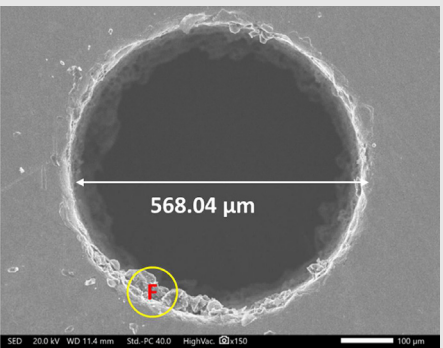
Fig. 4 (b) represents the TWR fluctuation with TRS. The graph illustrates that the TWR decreases when TRS increases from 0 to 1000. The WCu electrode has a lower TWR than other electrodes due to its greater melting point and low heat conductivity. Due to a lower melting point than WCu and WC, Cu exhibits a larger TWR. When TRS varied from 0 to 1000 rpm, the TWR decreased by 50.81%, 114.76% and 133.59%, for Cu, WCu and WC electrodes, respectively. TRS provides additional flushing for the μEDD by generating the centrifugal force in the dielectric fluid, removing the debris from the IEG and allowing a fresh dielectric fluid to the subsequent cycle. According to

studies, the carbon migrates from hydrocarbon dielectric fluids to the tool electrode's surface and deposits itself, preventing the electrode surface from wearing down. Huang et al. [45] discovered that increasing the TRS enhances the centrifugal force that eliminates carbon from electrode surfaces, increasing TWR.

The effect of TRS is substantial on the OC, as seen in Fig. 4 (c). The OC for various tool electrode materials lowers as TRS increases. The amount of flushing in the machined zone increases as the electrode rotating speed increases, ensuing in the quick elimination of debris and reducing the chances of resolidification of the melted metal on the newly cut surface. The WC electrode achieves the most negligible OC value of 0.006105 mm at 1000 rpm, which is 19.11% and 38.98% less than the WCu and Cu electrodes, respectively. The highest OC value of 0.06608 mm is achieved at 0 rpm by the Cu electrode, which is 6.73% and 29.55% higher than the WCu and WC electrodes, respectively.

Fig. 4 (d) shows that the HT value for the Cu, WCu and WC electrodes decreased by 357.67%, 442.72% and 448.64% with a

Table 9 – Surface quality of fabricated micro-holes with various electrodes at Low DE and High DE settings.

Electrode	Low discharge energy and stationary tool electrode (V = 80 V,C = 100 pF and TRS = 0 RPM)	High discharge energy and rotary tool electrode (V = 80 V C = 10000 pF and TRS = 0 RPM)
Cu	547.14 μm	601.31 μm
WCu	549.80 μm	599.80 μm
WC	527.16 μm	568.04 μm

rise in the TRS from 0 rpm to 1000 rpm. The WC electrode exhibits the lowest HT of 0.2777° at 1000 rpm, which is 53.47% and 9.08% higher than the Cu and WCu electrodes. It indicates that the HT is more sensitive to TRS. As the electrode speed increases, the dielectric fluid turbulence in IEG increases, causing material debris removed from the hole. This help to move the electrode in a downward direction producing a more accurate hole of a given size.
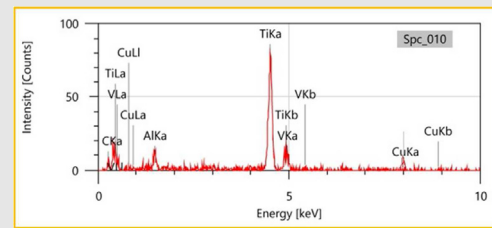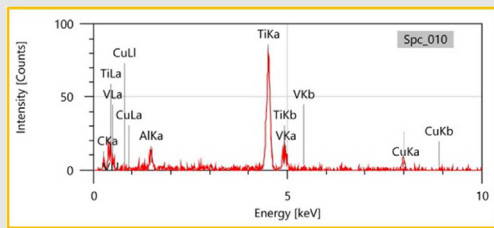
3.2.4. Surface quality and accuracy of microholes
An SEM machine was used to capture images of microholes from top surface of the workpiece. According to the literature, capacitance is the primary factor for surface texture changes during μEDD of Ti−6Al−4V. Therefore, six additional experiments were carried out at low DE and high DE settings to investigate the effect of capacitance on the quality and accuracy of holes.
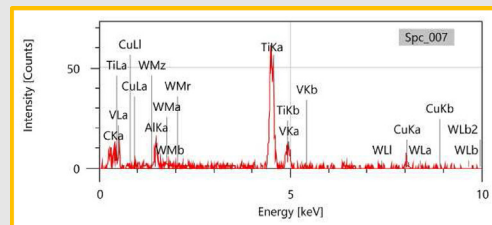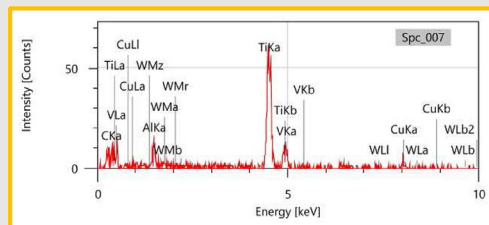
Table 10 − EDX of fabricated micro-holes with various electrodes at Low DE and High DE settings.

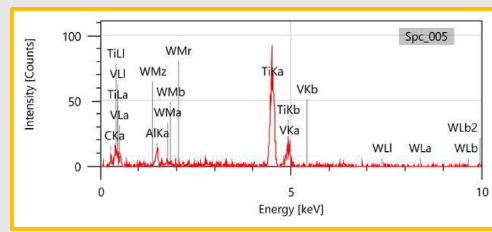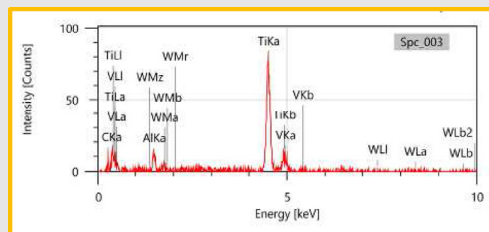| Electrode	Low discharge energy and stationary tool electrode (V = 80 V,C = 100 pF and TRS = 0 RPM)	High discharge energy and rotary tool electrode (V = 80 V C = 10000 pF and TRS = 0 RPM)
Cu		
WCu		
WC		

The microscopic images of micro-holes produced at low DE and high DE settings are displayed in Table 9. The deviation from the desired diameter of the hole (i.e. 500 μm) is also reported. It is evident by examining images of the micro-holes that the capacitance significantly impacts the precision and quality of the micro-holes manufactured. With the rise in capacitance value, the diameter of micro-holes was seen to be increasing, resulting in an increase in OC. At low capacitance values, a low volume of the workpiece will be removed per discharge, thereby creating finer craters. This resulted in a low OC compared to a high capacitance value.

Similarly, the discharge column constructed at high capacitance continues for longer than one at a small capacitance value, causing a higher ionization effect and widening micro-hole. At a high capacitance value, more burrs caused by the resolidification of debris and craters were seen on the hole's edge. It can be observed that the capacitance substantially impacted the surface quality of holes produced by μEDD. At a higher capacitance setting, the DE increased significantly, creating high pressure and temperature in the IEG. Craters were formed in μEDD due to actual discharge at the side wall

surface of the holes after machining. Besides that, it has also been discovered that as ERS increases, the OC of the generated micro-hole reduces, i.e. the diameter of the manufactured holes lowers.

During μEDM drilling, debris and melted metal become caught in the IEG under side flushing circumstances, resulting in an increased discharge column width. As a result, the diameter of micro-holes increases. The WCu tool electrode has a lower tool wear owing to its higher melting point. Table 9 shows the quality of the surface on the entry of micro-holes created by μEDD on Ti−6Al−4V with different control factor settings, illustrating the effect of discharge energy.

Table 10 represents the relative elemental analysis, performed using EDX examination, at entrance holes machined by the Cu, WCu, and WC tool electrodes. The EDX measurement revealed tool electrode material migration in produced holes. The percentage migration of carbon on the wall surface was discovered to be greater for the WCu electrode as compared to the Cu and WC electrodes. It is clear from Table 8 that the WCu electrode exhibits the highest MRR causing an

Table 11 — EDX comparison of micro-holes fabricated with copper, tungsten copper, and tungsten carbide electrodes.

Elements	For copper		For tungsten copper		For tungsten carbide	
	Low DE	High DE	Low DE	High DE	Low DE	High DE
Ti	75.01	73.27	75.09	72.15	78.15	77.37
V	6.64	5.63	6.44	5.98	5.74	5.58
Al	4.58	4.34	3.82	4.53	3.93	3.77
C	12.59	13.70	12.09	14.94	10.62	11.69
Cu	1.18	3.06	1.20	1.46	—	—
W	—	—	1.36	0.96	1.56	2.59

{Here, Low DE (V = 80 V, C = 100 pF, TRS = 0 RPM); High DE (V = 80 V, C = 10,000 pF, TRS = 0 RPM)}.

effective breakdown of dielectric fluid; due to this, carbon deposition will be more for the WCu electrode. Table 11 depicted carbon migration increased by 23.57% when capacitance increased from 0 pF to 10000 pF for the WCu electrode. Carbon migration for the Cu and WC electrodes showed 8.81% and 10.07% rise when the capacitance value was increased from 0 pF to 10000 pF.

4. Conclusion

This study presents a comparative study of the effects of Cu, WCu, and WC tool electrodes on micro-electric discharge drilling (μEDD) of Ti—6Al—4V alloy. The study investigated the impact of voltage, capacitance, and tool rotation speed (TRS) on key process response variables, including material removal rate (MRR), tool wear rate (TWR), overcut (OC), and hole taper (HT). The following interpretations are drawn based on results of this study.

- To achieve lower tool wear rate (TWR), a tool electrode with high melting point, poor electrical conductivity, and low thermal conductivity is recommended. The results showed that the WCu electrode had the lowest TWR compared to Cu and WC electrodes, with reductions of 73.27% and 57.53%, respectively, at the highest capacitance value. This suggests that WCu may be a suitable tool material for achieving greater accuracy and productivity in microhole fabrication.
- The WCu electrode had a 5.87% and 24.21% larger MRR than the Cu and WC electrodes, respectively, due to variations in the amount of heat produced in the IEG and the incidence of sparks. These results suggest that WCu may be a suitable tool material for achieving higher machining efficiency and productivity in the fabrication of microholes on the Ti-6Al-4V alloy.
- A high tool rotation play a significant role in reducing the OC by 88.24% and HT by 81.57% due to proper flushing of debris particles.
- The WC electrode depicted the smallest OC value of 0.052 mm and the smallest HT value of 1.4657° as compared to those for the Cu and WCu electrodes. The principal cause of this phenomenon is the thermal and electrical properties, and the melting point of the tool electrode material.

- Capacitance was found to be the most important process variable affecting MRR, TWR, OC, and HT for all three tool electrodes. High capacitance values are suitable for improving MRR, but they can have an adverse effect on TWR, OC, and HT.
- The EDX measurement revealed tool material migration to the hole surface. In addition, carbon deposition also found at hole surface.
- The WCu electrode showed the highest migration of carbon on the surface of the hole, particularly at high capacitance values, when compared to the Cu and WC electrodes.

Credit authorship contribution statement

Sachin S. Sawant: Conceptualization, technique, investigation, validation, formal analysis, research, data curation, and writing — original draft. *Sachin Patil*: Resources, validation, formal analysis, writing — review, and editing, Supervision. *Deepak Rajendra Unune*: Conceptualization, technique, validation, formal analysis, research, data curation, and writing — original draft. *Prasand Nazare*: Investigation, formal analysis, research, data curation. *Szymon Wojciechowski*: validation, formal analysis, writing — review, and editing.

Declaration of competing interest

The authors declare that they have no known competing financial interests or personal relationships that could have appeared to influence the work reported in this paper.

REFERENCES

[1] Mao X, Almeida S, Mo J, Ding S. The state of the art of electrical discharge drilling: a review. Int J Adv Manuf Technol 2022;121(5—6):2947—69. https://doi.org/10.1007/s00170-022-09549-7.

[2] Papazoglou EL, Karmiris-Obratański P, Leszczyńska-Madej B, Markopoulos AP. A study on electrical discharge machining of titanium Grade 2 with experimental and theoretical analysis. Sci Rep 2021;11(1):8971. https://doi.org/10.1038/s41598-021-88534-8.

[3] Youssef H, El-Hofy H. In: Non-traditional machining processes. 2013th, vols. 978—1—4471—5179—1. New York Dordrecht: Springer London Heidelberg; 2020. https://doi.org/10.1007/978-1-4471-5179-1.

[4] Hazra Sonakshi, Mohanty Shalini, Kumar Shakti, Basak Ranjit, Das Alok Kumar. Experimental investigation of powder mixed micro-electrical discharge drilling on SS304 substrate. Part 1 Mater Today Proc 2022;62:270—5. https://doi.org/10.1016/j.matpr.2022.03.258. ISSN 2214-7853.

[5] Abidi MH, Al-Ahmari AM, Umer U, Rasheed MS. Multi-objective optimization of micro-electrical discharge machining of nickel-titanium-based shape memory alloy using MOGA-II," Measurement. J Intern Measure Confeder 2018;125(April):336—49. https://doi.org/10.1016/j.measurement.2018.04.096.

[6] Ishfaq K, Rehman M, Wang Y. Toward the targeted material removal with optimized surface finish during EDM for the repair applications in dies and molds. Arabian J Sci Eng 2023;48:2653—69. https://doi.org/10.1007/s13369-022-07006-x.

[7] Dewangan S, Biswas CK, Gangopadhyay S. Influence of different tool electrode materials on EDMed surface integrity of AISI P20 tool steel. Mater Manuf Process 2014;29(11—12):1387—94. https://doi.org/10.1080/10426914.2014.930892.

[8] Lee SH, Li XP. Study of the effect of machining parameters on the machining characteristics in electrical discharge machining of tungsten carbide. J Mater Process Technol 2001;115(3):344—58. https://doi.org/10.1016/S0924-0136(01)00992-X.

[9] Singh S, Maheshwari S, Pandey PC. Some investigations into the electric discharge machining of hardened tool steel using different electrode materials. J Mater Process Technol 2004;149(1—3):272—7. https://doi.org/10.1016/j.jmatprotec.2003.11.046.

[10] Ishfaq K, Maqsood M, Mahmood M. Machining characteristics of various powder-based additives, dielectrics, and electrodes during EDM of micro-impressions: a comparative study. Int J Adv Manuf Technol 2022;123:1521—41. https://doi.org/10.1007/s00170-022-10254-8.

[11] Zhu G, Zhang Q, Wang K, Huang Y, Zhang J. Effects of different electrode materials on high-speed electrical discharge machining of W9Mo3Cr4V. Procedia CIRP 2018;68(April):64—9. https://doi.org/10.1016/j.procir.2017.12.023.

[12] Chandra Mouli A, Parameswara Rao CHVS, Deva Kumar MLS. Analysis and synthesis of influence of tool-electrode materials in electric discharge machining of M2 high-speed tool steel. Int J Mech Prod Eng Res Dev 2020;10(3):8361—70. https://doi.org/10.24247/ijmperdjun2020794.

[13] Che Haron CH, Ghani JA, Burhanuddin Y, Seong YK, Swee CY. Copper and graphite electrodes performance in electrical-discharge machining of XW42 tool steel. J Mater Process Technol 2008;201(1—3):570—3. https://doi.org/10.1016/j.jmatprotec.2007.11.285.

[14] Bhaumik M, Maity K. Effect of electrode materials on different EDM aspects of titanium alloy. Silicon 2019;11(1):187—96. https://doi.org/10.1007/s12633-018-9844-x.

[15] Zahoor S, Abdul-Kader W, Ishfaq K. Sustainability assessment of cutting fluids for flooded approach through a comparative surface integrity evaluation of IN718. Int J Adv Manuf Technol 2020;111(1—2):383—95. https://doi.org/10.1007/s00170-020-06130-y.

[16] Choudhary S, Kant K, Saini P. Analysis of MRR and SR with different electrode for SS 316 on die-sinking EDM using Taguchi technique. Global J Res Eng 2013;13(3):15—21.

[17] Rex NA, Vijayan K. Machining of microholes in Ti-6Al-4V by hybrid electro-discharge machining process. J Braz Soc Mech Sci Eng 2022;44:129. https://doi.org/10.1007/s40430-022-03428-8.

[18] Ishfaq Kashif, Waseem Muhammad Umair, Sana Muhammad. Investigating cryogenically treated electrodes' performance under modified dielectric(s) for EDM of Inconel (617). Mater Manuf Process 2022;37(16):1902—11. https://doi.org/10.1080/10426914.2022.2065016.

[19] D'Urso G, Merla C. Workpiece and electrode influence on micro-EDM drilling performance. Precis Eng 2014;38(4):903—14. https://doi.org/10.1016/j.precisioneng.2014.05.007.

[20] Sen G, Mondal SC. Investigation of the effect of copper, brass and graphite electrode on electrical discharge machining of mild steel grade IS2062. AIP Conf Proc 2020;2273. https://doi.org/10.1063/5.0024672.

[21] D'Urso G, Maccarini G, Ravasio C. Influence of electrode material in micro-EDM drilling of stainless steel and tungsten carbide. Int J Adv Manuf Technol 2016;85(9—12):2013—25. https://doi.org/10.1007/s00170-015-7010-9.

[22] Gopalakannan S, Senthilvelan T. Effect of electrode materials on electric discharge machining of 316 L and 17 - 4 PH stainless steels. J Miner Mater Char Eng 2012;11(7):685—90. https://doi.org/10.4236/jmmce.2012.117053.

[23] Unune DR, Nirala CK, Mali HS. Accuracy and quality of micro-holes in vibration assisted micro-electro-discharge drilling of Inconel 718," Measurement. J Intern Measure Confeder 2019;135:424—37. https://doi.org/10.1016/j.measurement.2018.11.067.

[24] Sapkal SU, Jagtap PS. Optimization of micro EDM drilling process parameters for titanium alloy by rotating electrode. Procedia Manuf 2018;20:119—26. https://doi.org/10.1016/j.promfg.2018.02.017.

[25] Hasçalik A, Çaydaş U. Electrical discharge machining of titanium alloy (Ti-6Al-4V). Appl Surf Sci 2007;253(22):9007—16. https://doi.org/10.1016/j.apsusc.2007.05.031.

[26] Jahan MP, Wong YS, Rahman M. A study on the fine-finish die-sinking micro-EDM of tungsten carbide using different electrode materials. J Mater Process Technol 2009;209(8):3956—67. https://doi.org/10.1016/j.jmatprotec.2008.09.015.

[27] Yadav US, Yadava V. Experimental investigation on electrical discharge drilling of Ti-6Al-4V alloy. Mach Sci Technol 2015;19(4):515—35. https://doi.org/10.1080/10910344.2015.1085316.

[28] Yilmaz O, Bozdana AT, Okka MA. An intelligent and automated system for electrical discharge drilling of aerospace alloys: inconel 718 and Ti-6Al-4V. Int J Adv Manuf Technol 2014;74(9—12):1323—36. https://doi.org/10.1007/s00170-014-6059-1.

[29] Joy N, Prakash S, Krishnamoorthy A, Antony A. Experimental investigation and analysis of drilling in Grade 5 Titanium alloy (Ti-6Al-4V). Mater Today Proc 2020;21(xxxx):335—9. https://doi.org/10.1016/j.matpr.2019.05.458.

[30] Zhu Z, Sui S, Sun J, Li J, Li Y. Investigation on performance characteristics in drilling of Ti6Al4V alloy. Int J Adv Manuf Technol 2017;93(1—4):651—60. https://doi.org/10.1007/s00170-017-0508-6.

[31] Mondol K, Azad MS, Puri AB. Analysis of micro-electrical discharge drilling characteristics in a thin plate of Ti—6Al—4 V. Int J Adv Manuf Technol 2013;76(1—4):141—50. https://doi.org/10.1007/s00170-013-5414-y.

[32] Barman S, Puri AB, Nagahanumaiah. Analysis of surface texture of high aspect ratio blind microholes on titanium alloy (Ti-6al-4v) in micro electrical discharge drilling. Solid State Phenom 2017;261:151—8. https://doi.org/10.4028/www.scientific.net/SSP.261.151. SSP.

[33] Rahul, Mishra DK, Datta S, Masanta M. Effects of tool electrode on EDM performance of Ti-6Al-4V. Silicon 2018;10(5):2263—77. https://doi.org/10.1007/s12633-018-9760-0.

[34] Plaza S, Sanchez JA, Perez E, Gil R, Izquierdo B, Ortegaa N, et al. Experimental study on micro EDM-drilling of Ti6Al4V using helical electrode. Precis Eng 2014;38(4):821—7. https://doi.org/10.1016/j.precisioneng.2014.04.010.

[35] Ahmad S, Lajis MA. Electrical discharge machining (EDM) of Inconel 718 by using copper electrode at higher peak current and pulse duration. IOP Conf Ser Mater Sci Eng 2013;50(1). https://doi.org/10.1088/1757-899X/50/1/012062.

[36] Moses MD, Jahan MP. Micro-EDM machinability of difficult-to-cut Ti-6Al-4V against soft brass. Int J Adv Manuf Technol 2015;81(5—8):1345—61. https://doi.org/10.1007/s00170-015-7306-9.

[37] Prasanna J, Rajamanickam S, Kumar OA, Karthick Raj G, Narayanan PVVS. MRR and TWR evaluation on electrical discharge machining of Ti-6Al-4V using tungsten: copper composite electrode. IOP Conf Ser Mater Sci Eng 2017;197(1). https://doi.org/10.1088/1757-899X/197/1/012087.

[38] Ay M, Çaydaş U, Hasçalik A. Optimization of micro-EDM drilling of inconel 718 superalloy. Int J Adv Manuf Technol 2013;66(5—8):1015—23. https://doi.org/10.1007/s00170-012-4385-8.

[39] Dewangan S, Deepak Kumar S, Kumar Jha S, Kumar Biswas C. Optimization of Micro-EDM drilling parameters of Ti—6Al—4V alloy. Mater Today Proc 2020;xxxx:2—6. https://doi.org/10.1016/j.matpr.2020.03.307.

[40] Selvarajan L, Manohar M, Udhaya kumar A, Dhinakaran P. Modelling and experimental investigation of process parameters in EDM of Si3N4-TiN composites using GRA-RSM. J Mech Sci Technol 2017;31(1):111—22. https://doi.org/10.1007/s12206-016-1009-5.

[41] Bin Wan Azhar WA, Saleh T. "Development and performance evaluation of modular RC-based power supply for micro-EDM". In: 2019 7th international conference on mechatronics engineering, ICOM 2019; 2019. p. 1—6. https://doi.org/10.1109/ICOM47790.2019.8952034.

[42] Kuppan P, Narayanan S, Rajadurai A. Effect of process parameters on material removal rate and surface roughness in electric discharge drilling of Inconel 718 using graphite electrode. Int J Manuf Technol Manag 2011;23(3—4):214—33. https://doi.org/10.1504/IJMTM.2011.045509.

[43] Akgün M. Performance analysis of electrode materials in electro discharge machining of monel K-500. Surf Topogr Metrol Prop 2022;10(3):35026. https://doi.org/10.1088/2051-672X/ac8d19.

[44] Singh R, Dvivedi A, Kumar P. EDM of high aspect ratio micro-holes on Ti-6Al-4V alloy by synchronizing energy interactions. Mater Manuf Process 2020;35(11):1188—1203, Aug. https://doi.org/10.1080/10426914.2020.1762207.

[45] Huang Y, Zhang Q, Xing Q, Yao Z, Li J. Effects of electrode rotational speed on processing performances of AISI 304 in micro-electrical discharge machining. Int J Adv Des Manuf Technol 2019;105(1):1665—74. https://doi.org/10.1007/s00170-019-04345-2.